

Crystallization and preliminary X-ray diffraction analysis of two N-terminal fragments of the DNA-cleavage domain of topoisomerase IV from *Staphylococcus aureus*. Corrigendum

Stephen B. Carr,^{a*} George Makris,^b Simon E. V. Phillips^a
and Christopher D. Thomas^a

^aAstbury Centre for Structural Molecular Biology, University of Leeds, Leeds LS2 9JT, England, and ^bOmega Mediation Hellas Ltd, Clinical and Pharma Consulting, 11525 N. Psychiko, Athens, Greece

Correspondence e-mail: bmsbc@bmb.leeds.ac.uk

A correction is made to a statement in the article by Carr *et al.* (2006), *Acta Cryst.* **F62**, 1164–1167.

Since the publication of our manuscript and deposition of coordinates (PDB code 2inr) we have learnt that our claim of a first report of the crystallization of a DNA-cleavage domain of a topoisomerase IV from a Gram-positive organism (Carr *et al.*, 2006) overlooked a poster abstract in the proceedings of the IUCr meeting in Florence (Laponogov *et al.*, 2005) announcing crystallization of a fragment of the A subunit of topoisomerase IV from *S. pneumoniae*. This structure has also recently been deposited (PDB code 2nov).

References

Carr, S.B., Makris, G., Phillips, S. E. V. & Thomas, C. D. (2006). *Acta Cryst.* **F62**, 1164–1167.

Laponogov, I., Veselkov, D., Sohi, M., Pan, X.-S., Fisher, M. & Sanderson, M. (2005). *Acta Cryst.* **A61**, C176.

Stephen B. Carr,^{a*} George Makris,^b Simon E. V. Phillips^a and Christopher D. Thomas^a

^aAstbury Centre for Structural Molecular Biology, University of Leeds, Leeds LS2 9JT, England, and ^bOmega Mediation Hellas Ltd, Clinical and Pharma Consulting, 11525 N. Psychiko, Athens, Greece

Correspondence e-mail:
 bmsbc@bmb.leeds.ac.uk

Received 11 October 2006

Accepted 23 October 2006

Crystallization and preliminary X-ray diffraction analysis of two N-terminal fragments of the DNA-cleavage domain of topoisomerase IV from *Staphylococcus aureus*

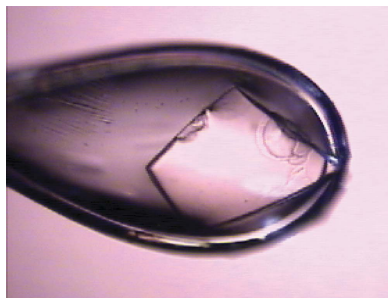
DNA topoisomerase IV removes undesirable topological features from DNA molecules in order to help maintain chromosome stability. Two constructs of 56 and 59 kDa spanning the DNA-cleavage domain of the *A* subunit of topoisomerase IV from *Staphylococcus aureus* (termed Gr1A56 and Gr1A59) have been crystallized. Crystals were grown at 291 K using the sitting-drop vapour-diffusion technique with PEG 3350 as a precipitant. Preliminary X-ray analysis revealed that Gr1A56 crystals belong to space group $P2_1$, diffract to a resolution of 2.9 Å and possess unit-cell parameters $a = 83.6$, $b = 171.5$, $c = 87.8$ Å, $\beta = 90.1^\circ$, while crystals of Gr1A59 belong to space group $P2_12_12$, with unit-cell parameters $a = 41.5$, $b = 171.89$, $c = 87.9$ Å. These crystals diffract to a resolution of 2.8 Å. This is the first report of the crystallization and preliminary X-ray analysis of the DNA-cleavage domain of a topoisomerase IV from a Gram-positive organism.

1. Introduction

DNA is prone to topological problems owing to its double-helical structure and the intertwining of its complementary strands. For example, during replication the unwinding of the chromosome forces adjacent regions of DNA to overwind and underwind, generating a superhelical strain (Wu *et al.*, 1988). The removal of this intermolecular strain is vital for the prevention of DNA tangling and knotting, which produces structures that can lead to the formation of double-stranded breaks in the DNA and chromosome instability (Kato *et al.*, 1990); furthermore, it is essential that circular daughter chromosomes of bacteria are disentangled at cell division. The resolution of such structures is performed by topoisomerase IV (topoIV), a type IIA DNA topoisomerase, which can remove these regions of unusual topology by passing one double-helical segment of DNA through another.

All bacterial type IIA topoisomerases are A_2B_2 heterotetramers containing three discrete subunit interfaces which open and close sequentially in response to ATP binding and hydrolysis in order to effect DNA transport (Wang, 1998). One segment of DNA (termed the gate segment) is initially bound by the *A* subunit, followed by the capture of a second strand (termed the transfer segment) by the *B* subunits as they bind ATP and dimerize. The dimerization and ensuing interaction with the *A* subunits triggers the cleavage of the gate segment. Subsequent hydrolysis of ATP causes the transfer segment to be passed through the DNA gate. DNA passage is followed by resealing of the gate segment and release of the transfer segment from the enzyme (Corbett & Berger, 2004).

Topoisomerases perform such a vital role in the maintenance of genetic stability within the cell that they are ideal drug targets and are the site of action of numerous antibacterial agents (Hooper, 2001). One class of inhibitor includes the quinolone antibiotics, which have proven to be highly effective against a variety of bacterial species (Oliphant & Green, 2002). These molecules bind to the *A* subunit and stabilize the topoisomerase–DNA complex formed during the catalytic turnover of the enzyme. The stalled topoisomerase complex then acts as a physical barrier to DNA replication. Collision of an active replication complex with the topoisomerase is thought to lead to the



© 2006 International Union of Crystallography
 All rights reserved

double-stranded breaks necessary for cell lethality (Drlica & Zhao, 1997), although the exact mechanism by which this occurs is unknown.

Topoisomerase IV has been shown to be the primary target for quinolones in Gram-positive species (Oliphant & Green, 2002), but currently structural information is only available for the DNA-cleavage domains of topoisomerases from eukaryotic (PDB code 1bgw; Berger *et al.*, 1996) and Gram-negative bacterial species (PDB codes 1ab4 and 1zvz; Morais-Cabral *et al.*, 1997; Corbett *et al.*, 2005). Here, we describe the crystallization and X-ray analysis of two different constructs of the A subunit of topoisomerase IV from *Staphylococcus aureus* (GrlA) with a view to gaining further insight into the mode of inhibition of quinolone antibiotics against this enzyme.

2. Materials and methods

2.1. Purification

Full details of the expression and purification are given elsewhere (Carr *et al.*, 2006). Briefly, the two constructs encompassing the N-terminal domains of *S. aureus* GrlA (accession code D67075) were generated by PCR from genomic DNA into the expression vector pET15b, such that 23 amino acids derived from the vector (including a hexahistidine tag) are fused to codons 25–491 or 1–491 of GrlA.

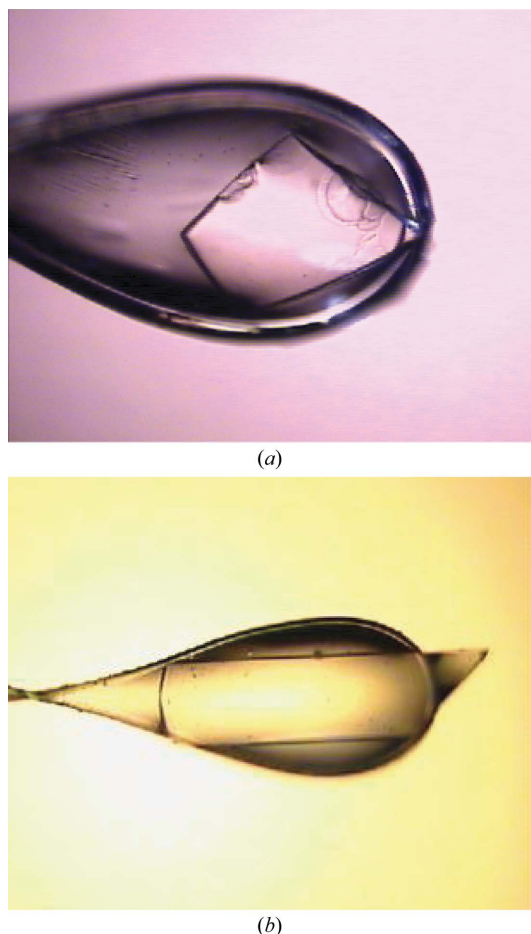


Figure 1
(a) A monoclinal crystal of GrlA56; typical dimensions are $400 \times 300 \times 20 \mu\text{m}$. (b) An orthorhombic crystal of GrlA59 mounted in a cryoloop prior to data collection; typical dimensions are $500 \times 150 \times 20 \mu\text{m}$.

Table 1

GrlA56 and GrlA59 X-ray diffraction data-collection statistics.

Values in parentheses are for the highest resolution bin.

	GrlA59	GrlA56
Space group	$P2_12_12$	$P2_1$
Unit-cell parameters (\AA , $^\circ$)	$a = 41.5$, $b = 171.89$, $c = 87.9$	$a = 83.6$, $b = 171.5$, $c = 87.8$, $\beta = 90.1$
Wavelength (\AA)	0.873	0.873
Resolution limits (\AA)	88–2.8 (2.95–2.8)	88–2.9 (3.06–2.9)
Matthews coefficient ($\text{\AA}^3 \text{Da}^{-1}$)	2.80	2.81
Molecules per ASU	1	4
Unique reflections	16113 (2308)	54736 (8090)
Completeness (%)	99.3 (99.3)	99.0 (99.0)
Multiplicity	3.6 (3.5)	3.7 (3.7)
$\langle I/\sigma(I) \rangle$	13.5 (3.1)	12.7 (2.7)
R_{merge}^\dagger (%)	8.4 (42.5)	8.7 (46.5)

$^\dagger R_{\text{merge}} = \sum_{\mathbf{h}} \sum_l |I_l - \langle I_{\mathbf{h}} \rangle| / \sum_{\mathbf{h}} \sum_l \langle I_{\mathbf{h}} \rangle$, where I_l is the l th observation of reflection \mathbf{h} and $\langle I_{\mathbf{h}} \rangle$ is the weighted average intensity for all observations l of reflection \mathbf{h} .

This leads to the generation of proteins with molecular weights of approximately 56 kDa (GrlA56) and approximately 59 kDa (GrlA59), respectively. Protein expression was performed in *Escherichia coli* B834 DE3 (plysS) cultures by incubation at 310 K for 3 h after the addition of IPTG to a final concentration of 0.5 mM. Cells were lysed by sonication in 50 mM Tris–HCl pH 7.5, 400 mM KCl, 10% (v/v) ethanediol and debris was removed by centrifugation (12 000g for 30 min). The resulting supernatant was loaded onto a column of HP chelating Sepharose (GE Healthcare), previously charged with nickel, and eluted with a 0–500 mM imidazole gradient. Protein-containing fractions were pooled and diluted with 50 mM Tris–HCl pH 7.5, 10% (v/v) ethanediol to a final KCl concentration of 75 mM. This material was then loaded onto a column of heparin Sepharose (GE Healthcare) pre-equilibrated with 50 mM Tris–HCl pH 7.5, 75 mM KCl, 10% (v/v) ethanediol. Protein was then eluted with a 0–1 M KCl gradient. Samples containing GrlA56 or GrlA59 were identified by absorbance at 280 nm and SDS–PAGE analysis. The purified proteins were extensively dialysed against 50 mM Tris–HCl pH 7.5, 400 mM KCl, 10% (v/v) ethanediol and concentrated to 5 mg ml^{-1} in an ultrafiltration cell (Millipore, 10 kDa cutoff).

2.2. Crystallization

Initial crystallization conditions were obtained by sparse-matrix screening (Jancarik & Kim, 1991) using the sitting-drop vapour-diffusion technique. Drops were prepared by mixing 0.5 μl protein solution with 0.5 μl screen solution using an Oryx6 liquid-handling robot (Douglas Instruments) and were equilibrated against a 100 μl reservoir of screen solution at 291 K. Initial crystals of both GrlA56 and GrlA59 appeared after 5 d from Index Screen solution No. 73 [100 mM Tris pH 8.5, 200 mM NaCl and 25% (w/v) PEG 3350; Hampton Research]. Streak-seeding into drops (2 μl protein and 2 μl 100 mM Tris pH 8.3–8.5, 200 mM NaCl and 12–16% PEG 3350) pre-equilibrated for 1–2 h against a 0.5 ml reservoir produced large diffraction-quality crystals for both constructs.

2.3. Data collection

Crystals were transferred into 100 mM Tris pH 8.5, 200 mM NaCl, 20% (w/v) PEG 3350 and 25% ethanediol prior to flash-cooling by immersion in liquid nitrogen. Data collection was performed at 100 K on station ID23.2, ESRF, France with a MAR CCD image-plate detector (MAR Research). Data were collected in multiple batches spanning 30° (0.5° oscillations), each separated by a translation of 50 μm along the long axis of the crystal, in order to minimize radiation damage. Diffraction data were integrated using *MOSFLM*

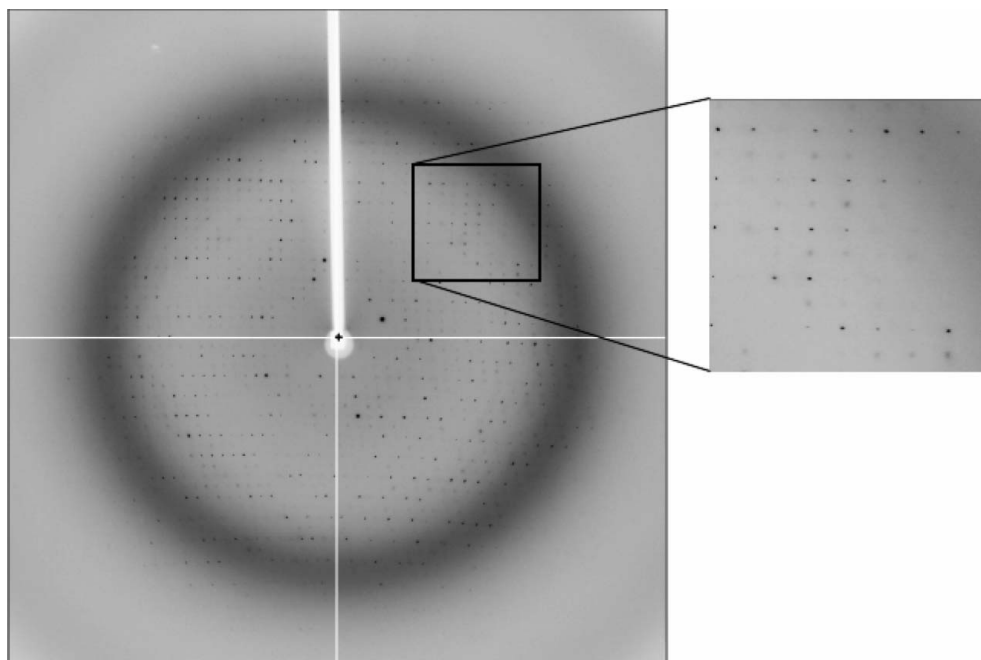


Figure 2 Diffraction pattern observed for GrlA56 crystals, with the differences in intensity between weak h_{odd} and strong h_{even} reflections highlighted.

(Leslie, 1992), followed by scaling and merging using *SCALA* (Evans, 1997). Further data analysis was performed using various programs from the *CCP4* program suite (Collaborative Computational Project, Number 4, 1994).

3. Results and discussion

Crystals of both protein fragments displayed a plate-like morphology and initially grew in tightly packed clusters. Streak-seeding proved the most effective method of producing large single crystals suitable for diffraction analysis (Figs. 1*a* and 1*b*). The diffraction images collected from crystals of GrlA56 were unusual in that they contained strong reflections when the h index was even and weak reflections when h was odd (Fig. 2).

The GrlA56 crystals belong to space group $P2_1$ (Table 1) and could contain between two and six copies of the construct per asymmetric unit, with four copies corresponding to a solvent content of 56% (Matthews, 1968). Calculation of a self-rotation function (Fig. 3) reveals the presence of orthorhombic pseudosymmetry, so the data were rescaled applying the pseudosymmetry ($P2_12_12$) indicated by inspection of systematic absences. Preliminary attempts at molecular replacement into the pseudo-cell using *AMoRe* (Navaza, 1994) were performed using the complete model of the 59 kDa fragment of DNA gyrase from *E. coli* (PDB code 1ab4; Morais Cabral *et al.*, 1997). This revealed a dimer within the asymmetric unit with an intermolecular twofold axis coincident with the crystallographic twofold. A slight distortion of the molecules that shifted the molecular twofold away from the crystallographic twofold would result in a lower symmetry monoclinic space group.

Applying a solvent content of 56% to the monoclinic cell suggests the presence of four molecules per asymmetric unit. Knowledge of the packing within the crystal suggests they should be arranged as a pair of dimers related by a direct translation of $a/2$ and each possessing a noncrystallographic twofold axis almost parallel to c . This packing also accounts for the presence of weak h_{odd} reflections in

the diffraction pattern, as the similar orientation of each pair of dimers results in the strong reflections corresponding to a unit cell with a cell edge of $a/2$ interspersed with weak intensities generated solely by the small differences between the two independent dimers. Further refinement of this model was severely impeded by the translational NCS relating each dimer within the asymmetric unit and this led to the redesign and production of the GrlA59 construct.

Crystals of GrlA59 belong to space group $P2_12_12$ (Table 1), contain one molecule per asymmetric unit and have a solvent content of 56%. The unit cell is related to that observed for GrlA56 crystals, but slight

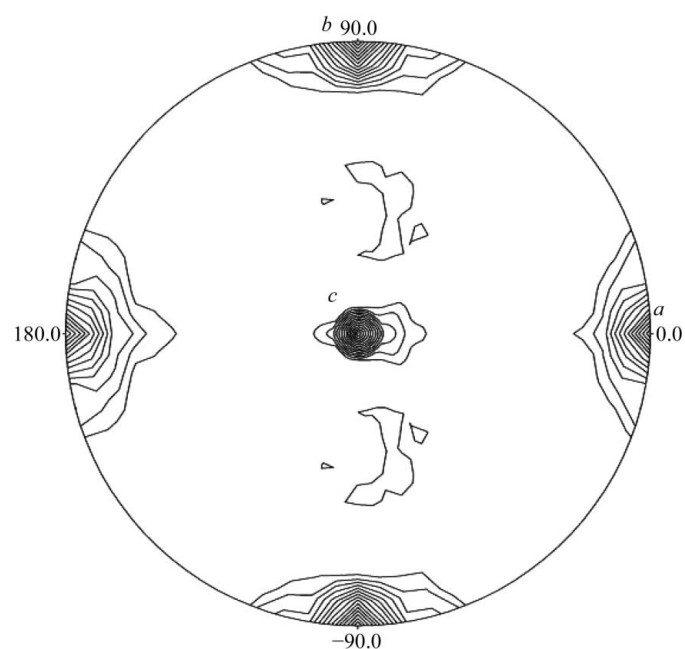


Figure 3 Self-rotation function ($\kappa = 180^\circ$) calculated for GrlA56 reveals orthorhombic pseudosymmetry within the monoclinic crystal lattice.

differences in packing have increased the order within the crystals, leading to the smaller unit cell and higher symmetry. It is possible that the additional residues at the N-terminus have created extra crystal contacts. It is likely that the orientation of the monomer within the asymmetric unit is such that the intermolecular twofold axis is parallel to *c*. Molecular replacement performed as previously described for GrIA56 confirm this assertion, generating a model suitable for rebuilding and refinement.

We would like to thank Val Sergeant for technical support and David Flot (ID23.2, ESRF) for assistance during data collection. We would also like to thank the Wellcome Trust for funding.

References

- Berger, J. M., Gamblin, S. J., Harrison, S. C. & Wang, J. C. (1996). *Nature (London)*, **379**, 225–232.
- Carr, S. B., Makris, G., Cove, J. H., Phillips, S. E. V. & Thomas, C. D. (2006). In preparation.
- Collaborative Computational Project, Number 4 (1994). *Acta Cryst.* **D50**, 760–763.
- Corbett, K. D. & Berger, J. M. (2004). *Annu. Rev. Biophys. Biomol. Struct.* **33**, 95–118.
- Corbett, K. D., Schoeffler, A. J., Thomsen, N. D. & Berger, J. M. (2005). *J. Mol. Biol.* **351**, 545–561.
- Drlica, K. & Zhao, X. L. (1997). *Microbiol. Mol. Biol. Rev.* **61**, 377–392.
- Evans, P. R. (1997). *Jnt CCP4/ESF-EACBM Newsl. Protein Crystallogr.* **33**, 22–24.
- Hooper, D. C. (2001). *Clin. Infect. Dis.* **32**, Suppl. 1, S9–S15.
- Jancarik, J. & Kim, S.-H (1991). *J. Appl. Cryst.* **24**, 409–411.
- Kato, J., Nishimura, Y., Imamura, R., Niki, H., Hirago, S. & Suzuki, H. (1990). *Cell*, **63**, 393–404.
- Leslie, A. G. W. (1992). *Jnt CCP4/ESF-EACBM Newsl. Protein Crystallogr.* **26**.
- Matthews, B. W. (1968). *J. Mol. Biol.* **33**, 491–497.
- Morais Cabral, J. H., Jackson, A. P., Smith, C. V., Shikotra, N., Maxwell, A. & Liddington, R. C. (1997). *Nature (London)*, **388**, 903–906.
- Navaza, J. (1994). *Acta Cryst.* **A50**, 157–163.
- Oliphant, C. M. & Green, G. M. (2002). *Am. Fam. Physician*, **65**, 455–464.
- Wang, J. C. (1998). *Q. Rev. Biophys.* **31**, 107–144.
- Wu, H. Y., Shyy, S., Wang, J. C. & Liu, L. F. (1988). *Cell*, **53**, 433–440.